

# FILIP: FINE-GRAINED INTERACTIVE LANGUAGE-IMAGE PRE-TRAINING

Lewei Yao<sup>1,2\*</sup> Runhui Huang<sup>3\*</sup> Lu Hou<sup>1\*</sup> Guansong Lu<sup>1</sup> Minzhe Niu<sup>1</sup>  
 Hang Xu<sup>1†</sup> Xiaodan Liang<sup>3†</sup> Zhenguo Li<sup>1</sup> Xin Jiang<sup>1</sup> Chunjing Xu<sup>1</sup>

<sup>1</sup>Huawei Noah’s Ark Lab

<sup>2</sup>Hong Kong University of Science and Technology

<sup>3</sup>Sun Yat-sen University

## ABSTRACT

Unsupervised large-scale vision-language pre-training has shown promising advances on various downstream tasks. Existing methods often model the cross-modal interaction either via the similarity of the global feature of each modality which misses sufficient information, or finer-grained interactions using cross/self-attention upon visual and textual tokens. However, cross/self-attention suffers from inferior efficiency in both training and inference. In this paper, we introduce a large-scale Fine-grained Interactive Language-Image Pre-training (FILIP) to achieve finer-level alignment through a cross-modal late interaction mechanism, which uses a token-wise maximum similarity between visual and textual tokens to guide the contrastive objective. FILIP successfully leverages the finer-grained expressiveness between image patches and textual words by modifying only contrastive loss, while simultaneously gaining the ability to pre-compute image and text representations offline at inference, keeping both large-scale training and inference efficient. Furthermore, we construct a new large-scale image-text pair dataset called FILIP300M for pre-training. Experiments show that FILIP achieves state-of-the-art performance on multiple downstream vision-language tasks including zero-shot image classification and image-text retrieval. The visualization on word-patch alignment further shows that FILIP can learn meaningful fine-grained features with promising localization ability.

## 1 INTRODUCTION

Large-scale Vision-Language Pre-training (VLP) models like CLIP (Radford et al., 2021) and ALIGN (Jia et al., 2021) have recently demonstrated success across various downstream tasks. They learn visual and textual representations from millions of image-text pairs collected from the Internet and show superior zero-shot ability and robustness. The core technique of these models lies in the global contrastive alignment of the images and texts through a dual-stream model. Such architecture is inference-efficient for downstream tasks like retrieval because the encoders for the two modalities can be decoupled and the image or text representations can be pre-computed offline. However, CLIP and ALIGN model the cross-modal interaction via solely the similarity of the global feature of each modality, lacking the ability of capturing finer-level information like the relationship between visual objects and textual words. In this paper, we develop a simple yet efficient cross-modal finer-grained interaction mechanism for large-scale VLP.

To achieve finer-grained cross-modal interaction, previous methods mainly exploited two kinds of methods. (1) One line of work (Chen et al., 2020; Li et al., 2020b; Dong et al., 2021; Li et al., 2021b; Zhang et al., 2021; Zhan et al., 2021) uses a pre-trained object detector to extract region-of-interest (ROI) features from images, and then fuses it with the paired text through a VLP model. This design complicates the pre-training due to pre-computing and storing a large number of ROI features. In addition, the zero-shot ability of these approaches is usually limited by the predefined number of classes and their performance is also restricted by the quality of the detector. (2) Another line of

\*Equal contribution

†Corresponding authors: xu.hang@huawei.com, xdliang328@gmail.com

work (Li et al., 2021a; Kim et al., 2021) enforces the token-wise or patch-wise representations from both modalities into the same space and models these finer-grained interactions via cross-attention (Li et al., 2021a) or self-attention (Kim et al., 2021). However, these methods are usually less efficient in terms of both training and inference. In particular, during training, cross-attention in (Li et al., 2021a) requires to be performed in an encoder-decoder structure, while the complexity of the self-attention (Kim et al., 2021) grows quadratically with the length of the prolonged concatenated sequences of both modalities. During inference, the data from both modalities are intertwined to compute the cross-attention or self-attention, and can not be pre-computed offline as dual-stream models like CLIP and ALIGN. This can be less efficient for downstream tasks like image/text retrieval and image classification.

In this paper, we propose a large-scale Fine-grained Interactive Language-Image Pre-training framework named FILIP to address these limitations. Inspired by Khattab & Zaharia (2020), we model the fine-grained semantic alignment through a novel cross-modal late interaction mechanism in the contrastive loss, instead of using cross or self-attention. Specifically, our fine-grained contrastive learning uses a token-wise maximum similarity between visual and textual tokens to guide the contrastive objective. In this way, FILIP successfully leverages the finer-grained expressiveness among image patches and textual words while simultaneously gaining the ability to pre-compute image and text representations offline. Unlike Khattab & Zaharia (2020), we discard the padded tokens and use average instead summation of token-wise maximum similarities when computing the image-text alignment, which enhances the cross-modal representation learning and stabilizes training. Furthermore, we construct a large-scale pre-training dataset named FILIP300M from the Internet. Data cleaning and image-text data augmentation are also explored and proved useful in this work.

Extensive experiments show that by effectively learning fine-grained representations, FILIP achieves state-of-the-art performance on multiple downstream vision-language tasks, including zero-shot image classification and image-text retrieval. For example, FILIP reaches 77.1% top-1 accuracy for zero-shot ImageNet classification, surpassing CLIP with less training data. Visualizations on word-patch alignment further show that FILIP learns meaningful finer-grained features with promising localization ability.

## 2 RELATED WORK

**Vision-Language Pre-training Models.** The pre-train-and-fine-tune scheme has achieved great success in the domains of natural language processing (Devlin et al., 2019; Brown et al., 2020) and computer vision (Dosovitskiy et al., 2020). It is then naturally extended to a joint cross-modal domain of Vision-and-Language Pre-training (VLP). The pre-training datasets of recent VLP models include publically available datasets like YFCC100M (Thomee et al., 2016) and CC12M (Chang-pinyo et al., 2021), as well as larger-scale datasets with more than 100M samples in CLIP (Radford et al., 2021) and ALIGN (Jia et al., 2021), which are shown to be even more powerful. The pre-training tasks of VLP models can be categorized into two categories: image-text contrastive learning task and Language Modeling (LM) based tasks: (i) CLIP (Radford et al., 2021), ALIGN (Jia et al., 2021) and UNIMO (Li et al., 2021b) make use of cross-modal contrastive learning which aligns the textual and visual information into a unified semantic space; (ii) VisualBERT (Li et al., 2019), UNITER (Chen et al., 2020), M6 (Lin et al., 2021), and DALL-E (Ramesh et al., 2021) employ LM-like objectives, including both masked LM (e.g., Masked Language/Region Modeling), and autoregressive LM (e.g., image captioning, text-grounded image generation). On the other hand, some methods rely on a pre-trained object detection model such as Faster-RCNN (Ren et al., 2015) to extract image regional features offline, which requires extra labeled bounding-box data and makes the approach less scalable. Recent efforts such as SOHO (Huang et al., 2021) and SimVLM (Wang et al., 2021) try to eliminate this burden via visual dictionary or PrefixLM (Raffel et al., 2020). In this paper, we directly learn fine-grained vision-language representations in an end-to-end and simpler manner while maintaining the benefit of inference efficiency.

**Multi-Modality Interaction Mechanism.** The core of vision-language pre-training models lies in modeling the interaction between the two modalities. There are mainly two types of cross-modal interaction architectures: single-stream and dual-stream models. Single-stream models like VisualBERT (Li et al., 2019) and ViLT (Kim et al., 2021) directly concatenate the patch-wise or regional visual features and textual embeddings and feed them to the transformer-based model. Dual-stream

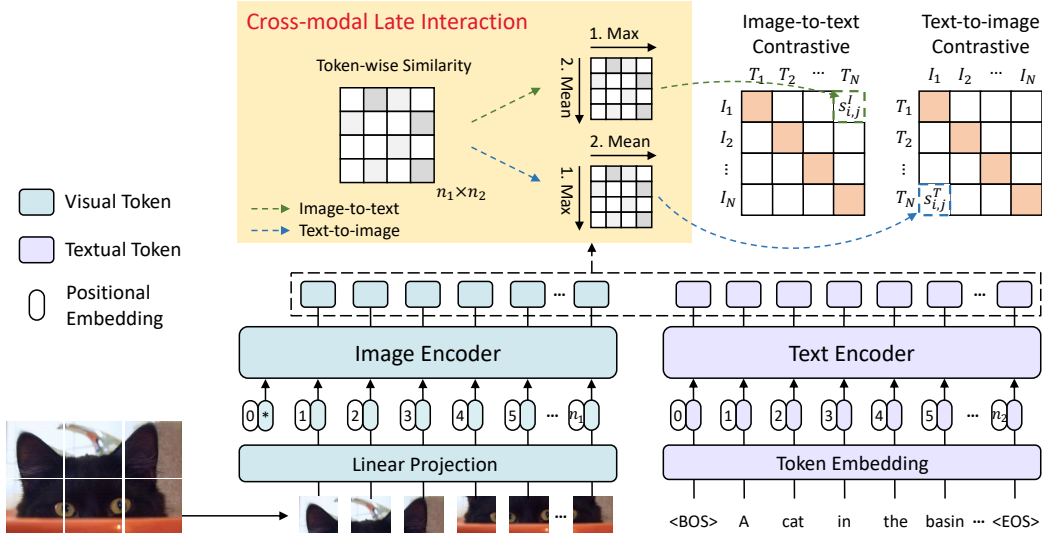


Figure 1: Overall architecture of FILIP, a dual-stream model with Transformer-based image and text encoders. On top of the image and text encoders, the representations of textual tokens and visual tokens are linearly projected to the multi-modal joint space. A novel fine-grained contrastive learning equipped with cross-modal late interaction is proposed, which uses a token-wise maximum similarity between visual and textual tokens.

models such as ViLBERT (Lu et al., 2019) and CLIP (Radford et al., 2021) have separate encoders for different modalities. This allows flexible use of different models for different modalities, and efficient inference for downstream tasks like image-text retrieval, through the ability of decoupling the encoders and pre-compute image/text features offline. In this paper, while following the dual-stream approach for its flexible and efficient inference, we further propose a new multi-modal interaction mechanism to capture the fine-grained representations.

### 3 METHOD

In this paper, we propose a new cross-modal pre-training model that excels in fine-grained interaction between image encoder and text encoder for mining more detailed semantic alignment, named as FILIP, as shown in Figure 1. Particularly, FILIP is a dual-stream model with Transformer-based image and text encoders. For the visual modality, the image encoder is a Vision Transformer (Dosovitskiy et al., 2020) which takes the concatenation of an extra [CLS] token embedding and linearly projected image patches as input. For the textual modality, following Radford et al. (2021), we use the lower-cased byte pair encoding (BPE) (Sennrich et al., 2016b) with a vocabulary size of 49,408 to tokenize the text. Each text sequence starts with [BOS] token and ends with [EOS] token. After the word embedding layer, the token embeddings are fed into a modified decoder-only Transformer model as in (Radford et al., 2019). On top of the image and text encoders, the representations of textual tokens and visual tokens are linearly projected to the multi-modal common space, and are separately L2-normalized. Different from existing dual-stream models (e.g., CLIP and ALIGN) which models cross-modal interaction via only the global features of the entire image and text sequence, we introduce a novel fine-grained contrastive learning objective equipped with cross-modal late interaction which takes into account the fine-grained interaction between image patches and textual tokens, detailed in Section 3.1.

#### 3.1 FINE-GRAINED CONTRASTIVE LEARNING

Contrastive representation learning has recently been found to learn better representations than its predictive counterpart in both visual (Tian et al., 2020) and vision-language cross-modal pre-training (Radford et al., 2021). Under a general formulation of cross-modal contrastive learning (Radford et al., 2021), we want to learn encoders  $f_\theta$  for image data  $\mathcal{I}$  and  $g_\phi$  for text data  $\mathcal{T}$  such that, given an image  $x^I \in \mathcal{I}$ , and a text  $x^T \in \mathcal{T}$ , the encoded representations  $f_\theta(x^I)$  and  $g_\phi(x^T)$  are close if they are related and far apart if not, under a distance metric. In each training batch, we sample  $b$

image-text pairs  $\{\mathbf{x}_k^I, \mathbf{x}_k^T\}_{k=1}^b$ . For image  $\mathbf{x}_k^I$  in image-text pair  $\{\mathbf{x}_k^I, \mathbf{x}_k^T\}$ ,  $\mathbf{x}_k^T$  is its positive, while the other texts will be used as in-batch negatives. The image-to-text contrastive loss  $\mathcal{L}_k^I$  for  $\mathbf{x}_k^I$  can then be formulated as

$$\mathcal{L}_k^I(\mathbf{x}_k^I, \{\mathbf{x}_j^T\}_{j=1}^b) = -\frac{1}{b} \log \frac{\exp(s_{k,k}^I)}{\sum_j \exp(s_{k,j}^I)},$$

where  $s_{k,j}^I$  denotes the similarity of the  $k$ -th image to the  $j$ -th text. Similarly, the text-to-image contrastive loss for  $\mathbf{x}_k^T$  is

$$\mathcal{L}_k^T(\mathbf{x}_k^T, \{\mathbf{x}_j^I\}_{j=1}^b) = -\frac{1}{b} \log \frac{\exp(s_{k,k}^T)}{\sum_j \exp(s_{j,k}^T)}.$$

The total loss of this mini-batch can be represented by

$$\mathcal{L} = \frac{1}{2} \sum_{k=1}^b (\mathcal{L}_k^I + \mathcal{L}_k^T). \quad (1)$$

### 3.1.1 CROSS-MODAL LATE INTERACTION

From the contrastive loss (1), the cross-modal interaction is reflected in how we compute the similarities  $s_{i,j}^I$  and  $s_{i,j}^T$  for the  $i$ -th image and  $j$ -th text. Previous methods like CLIP (Radford et al., 2021) and ALIGN (Jia et al., 2021) simply encode each image or text separately to a global feature i.e.,  $f_\theta(\mathbf{x}_i^I) \in \mathbb{R}^d$  and  $g_\phi(\mathbf{x}_j^T) \in \mathbb{R}^d$ , and compute these two similarities as

$$s_{i,j}^I = s_{i,j}^T = f_\theta(\mathbf{x}_i^I)^\top g_\phi(\mathbf{x}_j^T), \quad (2)$$

neglecting finer-grained interactions (e.g., word-patch alignment) between the two modalities. To alleviate this problem, while simultaneously maintain the training and inference efficiency of dual-stream models, we apply a cross-modal late interaction inspired by Khattab & Zaharia (2020) to model the token-wise cross-modal interaction.

Specifically, denote  $n_1$  and  $n_2$  as the number of (non-padded) tokens of the  $i$ -th image and  $j$ -th text, respectively, and the corresponding encoded features are  $f_\theta(\mathbf{x}_i^I) \in \mathbb{R}^{n_1 \times d}$  and  $g_\phi(\mathbf{x}_j^T) \in \mathbb{R}^{n_2 \times d}$ . For the  $k$ -th visual token, we compute its similarities with all textual tokens of  $\mathbf{x}_j^T$ , and use the largest one

$$\max_{0 \leq r < n_2} [f_\theta(\mathbf{x}_i^I)]_k^\top [g_\phi(\mathbf{x}_j^T)]_r \quad (3)$$

as its token-wise maximum similarity with  $\mathbf{x}_j^T$ . We then use the average token-wise maximum similarity of all non-padded tokens in the image (resp. text) as the similarity of an image to a text (resp. a text to an image). The similarity of the  $i$ -th image to the  $j$ -th text can thus be formulated as:

$$s_{i,j}^I(\mathbf{x}_i^I, \mathbf{x}_j^T) = \frac{1}{n_1} \sum_{k=1}^{n_1} [f_\theta(\mathbf{x}_i^I)]_k^\top [g_\phi(\mathbf{x}_j^T)]_{m_k^I}, \quad (4)$$

where  $m_k^I = \arg \max_{0 \leq r < n_2} [f_\theta(\mathbf{x}_i^I)]_k^\top [g_\phi(\mathbf{x}_j^T)]_r$ . Similarly, the similarity of the  $j$ -th text to the  $i$ -th image is

$$s_{i,j}^T(\mathbf{x}_i^I, \mathbf{x}_j^T) = \frac{1}{n_2} \sum_{k=1}^{n_2} [f_\theta(\mathbf{x}_i^I)]_{m_k^T}^\top [g_\phi(\mathbf{x}_j^T)]_k, \quad (5)$$

where  $m_k^T = \arg \max_{0 \leq r < n_1} [f_\theta(\mathbf{x}_i^I)]_r^\top [g_\phi(\mathbf{x}_j^T)]_k$ . Note that  $s_{i,j}^I(\mathbf{x}_i^I, \mathbf{x}_j^T)$  in Equation (4) does not necessarily equal  $s_{i,j}^T(\mathbf{x}_i^I, \mathbf{x}_j^T)$  in Equation (5).

**Remark 1** Intuitively, the token-wise maximum similarity in Equation (3) means that for each image patch, we find its most similar textual token. Similarly, for each textual token, we also find its closest image patch. By applying this to the similarity calculation in (4) and (5) for contrastive loss (1), the dual-stream model learns fine-grained alignment between image patches and textual tokens.

The original late interaction mechanism in (Khattab & Zaharia, 2020) computes the relevance score of a document to a query *padded with mask tokens*, as a *sum* of token-wise maximum similarities, and is optimized via a *pairwise* softmax cross-entropy loss. Though inspired from Khattab & Zaharia (2020), our proposed cross-modal late interaction differs in several aspects. Firstly, we exclude the padded textual tokens when computing the similarity, as they harm the performance. We speculate that this is because these padded tokens also learn textual representations and will mislead the model to align image patches to these meaningless padded tokens rather than meaningful non-padded words. Secondly, when computing similarities (4) and (5), we use the average of the token-wise maximum similarities instead of summation in (Khattab & Zaharia, 2020). This is because the number of non-padded tokens varies from text to text, and this summation over all non-padded tokens can have quite different magnitudes, leading to less stabilized training and worse final performance. Thirdly, we optimize the late interaction mechanism via a contrastive loss (1) which is found powerful vision-language pre-training (Radford et al., 2021) instead of the original pairwise loss in (Khattab & Zaharia, 2020).

**Training Efficiency.** Though the cross-modal late interaction is able to capture finer-grained features compared with the original loss, it relies on the token-wise representations of both modalities, and can be inefficient in terms of communication, memory and computation, especially when the batch size is large. To alleviate this problem, we utilize several methods. Firstly, we reduce the embedding size to 256. Besides, we reduce the precision of the last-layer features of both modalities from fp32 to fp16 before node communication in a distributed learning setting, and perform the multiplication in Equations (4) and (5) under the reduced precision. In addition, since the complexity of similarity calculation scales with the sequence length of textual tokens and image patches, for each image (resp. text), we select the 25% tokens with the highest token-wise maximum similarity score (Equation (3)) among all texts (resp. images) in the same local worker before node communication, based on the intuition that each sample can be represented by a few of the most representative tokens. Effects of these modifications are studied in Section 4.4.

### 3.1.2 PROMPT ENSEMBLE AND TEMPLATES

Due to the problem of polysemy and inconsistency with the pre-training process, following Radford et al. (2021), we also use prompt templates to augment the original label for some downstream tasks. For visualizations, for simplicity, we use only one prompt template across the paper, i.e. “a photo of a {label}.” as Radford et al. (2021). For other experiments, we report results using prompt ensemble following Radford et al. (2021). When multiple prompts are allowed, the token-wise representations of different prompt templates for the same class label are different, and can not be summed together to form a mean textual representation as in (Radford et al., 2021). Thus, instead of ensembling different prompt templates by their mean textual representation, we ensemble them by their mean token-wise similarity. Specifically, suppose there are  $C$  prompt templates, each label is augmented to  $C$  different texts  $x_1^T, x_2^T, \dots, x_C^T$ . The similarity between an image  $x^I$  and this label is computed as  $\frac{1}{C} \sum_{c=1}^C s_c^I(x^I, x_c^T)$ , where  $s_c^I$  is defined in Equation (4).

We use a unified rule-based method inspired by Radford et al. (2018) to construct prompt templates for image classification tasks. Specifically, each template consists of four components:

$$[\text{prefix}] \{\text{label}\}, [\text{category description}]. [\text{suffix}]. \quad (6)$$

Here, the “[prefix]” is an in-context description like “a photo of a” similar as Radford et al. (2021); “label” is a class label of the dataset; “[category description]” describes the category which is found helpful for some fine-grained image classification datasets (Radford et al., 2021), e.g., “a type of pet” for dataset Oxford-IIIT Pets. An interesting finding is that, adding a suffix that includes the reference word “it” (e.g., “I like it.”) at the end of the prompt empirically improves the zero-shot classification performance of the proposed model. We speculate this is because the reference word “it” strengthens the fine-grained cross-modal alignment, as it can also be aligned to image patches of the target object. Detailed prompt templates for different datasets can be found in Appendix A.4.

### 3.2 IMAGE AND TEXT AUGMENTATION

To obtain better generalization and data-efficiency of the model, we perform data augmentation on both images and texts during the pre-training phase to construct more image-text pairs. We apply AutoAugment (Krizhevsky et al., 2012; Sato et al., 2015; Cubuk et al., 2019; Hoffer et al., 2020)

Table 1: Top-1 accuracy(%) of zero-shot image classification on 12 datasets. Our FILIP can boost 3~5% accuracy on average.

	CIFAR10	CIFAR100	Caltech101	StanfordCars	Flowers102	Food101	SUN397	DTD	Aircrafts	OxfordPets	EuroSAT	ImageNet	Average
CLIP-ViT-B/32	91.3	65.1	87.9	59.4	66.7	84.4	63.2	44.5	21.2	87.0	49.4	63.2	65.3
FILIP <sub>base</sub> -ViT-B/32	86.9	65.5	91.9	55.4	85.3	82.8	69.1	49.3	57.2	88.1	49.9	68.8	<b>70.9</b> <sup>+5.6</sup>
CLIP-ViT-L/14	96.2	77.9	92.6	77.3	78.7	92.9	67.7	55.3	36.1	93.5	59.9	75.3	75.3
FILIP <sub>large</sub> -ViT-L/14	95.7	75.3	93.0	70.8	90.1	92.2	73.1	60.7	60.2	92	59.2	77.1	<b>78.3</b> <sup>+3.0</sup>

for image augmentation, following the SOTA vision recognition methods (Touvron et al., 2021; Xie et al., 2020b). To ensure the augmented texts are semantically similar as the original one, for text augmentation, we rewrite the original text using back-translation (Xie et al., 2020a; Sennrich et al., 2016a). Specifically, the texts are first translated to the target language and then translated back to the source language. We choose German and Russian as the target language and get extra two texts for each image-text pair. When constructing a batch of image-text pairs during the pre-training, the text of each image-text pair is randomly sampled from the three candidate texts, i.e., the original text and two back-translated texts.

### 3.3 PRE-TRAINING DATASET

A sufficiently large image-text dataset is a prerequisite for vision-language pre-training. Recent CLIP (Radford et al., 2021) and ALIGN (Jia et al., 2021) construct datasets with 400M and 1800M image-text pairs, respectively. In this work, we also construct a large-scale dataset called FILIP300M, which consists of 300M image-text pairs and covers board vision and language concepts. Specifically, we collect image-text pairs from the Internet, and apply the following image- and text-based filtering rules to clean data. For image-based filtering, we remove the images whose shorter dimension is smaller than 200 pixels and the aspect ratio is larger than 3. For text-based filtering, we keep only English texts, and exclude the meaningless ones, e.g., img\_0.jpg. We also discard image-text pairs whose texts are repeated for over 10 times. Besides, we also use 3 public datasets, including Conceptual Captions 3M (CC3M) (Sharma et al., 2018), Conceptual 12M (CC12M) (Changpinyo et al., 2021) and Yahoo Flickr Creative Commons 100M (YFCC100M) (Thomee et al., 2016). We apply the same filtering rules on YFCC100M. Finally, we use about 340M image-text pairs for pre-training. Despite using a smaller training dataset than CLIP and ALIGN, our models still outperform them in most down-stream tasks (see Section 4).

## 4 EXPERIMENTS

### 4.1 EXPERIMENTAL SETUP

**Model Architectures.** We train two models from scratch, i.e., FILIP<sub>base</sub> and FILIP<sub>large</sub>. The model architectures follow CLIP (Radford et al., 2021), i.e., the image encoder is ViT-B/32 for FILIP<sub>base</sub> and ViT-L/14 for FILIP<sub>large</sub>. More details can be found in Appendix A.2.

**Pre-training Details.** To save memory and scale up the batch size, automatic mixed-precision (Micikevicius et al., 2018) and gradient checkpoint (Griewank & Walther, 2000; Chen et al., 2016) are used. The input images are resized to  $224 \times 224$  resolution during pre-training and the maximum length of the text is limited to 77 tokens following Radford et al. (2021). The training is mainly conducted on Nvidia V100 GPUs and Ascend Cards. FILIP<sub>base</sub> is trained on 128 cards about 9 days and FILIP<sub>large</sub> takes about 24 days to train on 192 cards. Unless otherwise specified, we use FILIP<sub>large</sub> to compare with other methods and FILIP<sub>base</sub> for ablation. We train both models using the LAMB optimizer (You et al., 2020) and cosine learning rate schedule (Loshchilov & Hutter, 2016) with a linear warmup. Weight decay regularization is applied to all parameters except bias, layer normalization, token embedding, positional embedding and temperature in contrastive loss. Detailed values of hyperparameters for different datasets and models can be found in Appendix A.2.

Table 2: Results of zero-shot image-text retrieval on Flickr30K and MSCOCO datasets. The last two rows (marked with \*) report the zero-shot results on Flickr30K dataset of model fine-tuned on MSCOCO dataset, following the setting of ALBEF (Li et al., 2021a).

	Flickr30K						MSCOCO					
	image-to-text			text-to-image			image-to-text			text-to-image		
	R@1	R@5	R@10	R@1	R@5	R@10	R@1	R@5	R@10	R@1	R@5	R@10
Unicoder-VL	64.3	85.8	92.3	48.4	76.0	85.2	—	—	—	—	—	—
ImageBERT	70.7	90.2	94.0	54.3	79.6	87.5	44.0	71.2	80.4	32.3	59.0	70.2
UNITER	83.6	95.7	97.7	68.7	89.2	93.9	—	—	—	—	—	—
CLIP	88.0	98.7	99.4	68.7	90.6	95.2	58.4	81.5	88.1	37.8	62.4	72.2
ALIGN	88.6	98.7	99.7	<b>75.7</b>	<b>93.8</b>	<b>96.8</b>	58.6	83.0	89.7	45.6	69.8	78.6
<b>FILIP</b>	<b>89.8</b>	<b>99.2</b>	<b>99.8</b>	75.0	93.4	96.3	<b>61.3</b>	<b>84.3</b>	<b>90.4</b>	<b>45.9</b>	<b>70.6</b>	<b>79.3</b>
ALBEF*	94.1	99.5	99.7	82.8	96.3	98.1	—	—	—	—	—	—
<b>FILIP*</b>	<b>95.4</b>	<b>99.8</b>	<b>100.0</b>	<b>84.7</b>	<b>97.0</b>	<b>98.7</b>	—	—	—	—	—	—

## 4.2 ZERO-SHOT IMAGE CLASSIFICATION

In this section, we evaluate our proposed FILIP on the zero-shot image classification task. We compare our FILIP with CLIP (Radford et al., 2021) on 12 downstream classification datasets, using the same evaluation setting as in CLIP. As described in Section 3.1.2, we apply a set of prompts for each dataset and ensemble them to get the final results, see Appendix A.4 for details. We only compare the zero-shot performance with CLIP here as ALIGN does not release its model and the related performances are not reported in their paper.

Table 1 shows the results on 12 datasets. Despite using less training data (340M vs. 400M), both FILIP<sub>base</sub> and FILIP<sub>large</sub> considerably outperform their CLIP counterparts in terms of average top-1 accuracy over 12 datasets, i.e., achieving absolute improvements of 5.6% and 3.0%, respectively. In particular, our FILIP surpasses CLIP on ImageNet, the largest dataset among 12 datasets. FILIP also achieves substantial performance gains on some domain-specific datasets, e.g., for Aircrafts, the two FILIP models reach a 30% improvement over CLIP on average. We speculate this is because, unlike CLIP which aggregates the information of the whole image into the representation of the [CLS] token, our proposed FILIP model focuses more on the target object by directly aligning the image patches corresponding to the target object with the textual tokens corresponding to the class label (visualizations of word-patch alignment are in Section 4.5).

## 4.3 IMAGE-TEXT RETRIEVAL

Image-text retrieval consists of two sub-tasks: image-to-text retrieval and text-to-image retrieval. We evaluate our FILIP model on two retrieval benchmark datasets: Flickr30K (Plummer et al., 2015) and MSCOCO (Lin et al., 2014), under both zero-shot and fine-tuned settings. More details of experimental setting can be found in Appendix A.2.

Tables 2 and 3 show the results of zero-shot and fine-tuned image-text retrieval, respectively. We compare our FILIP model against methods with complex attention layers including Unicoder-VL (Li et al., 2020a), ImageBERT (Qi et al., 2020), UNITER (Chen et al., 2020), VILLA (Gan et al., 2020), ERNIE-ViL (Yu et al., 2021), Oscar (Li et al., 2020b), VinVL (Zhang et al., 2021), ALBEF (Li et al., 2021a), and methods trained on larger-scale image-text datasets including CLIP (Radford et al., 2021) and ALIGN (Jia et al., 2021). As we can see, FILIP achieves state-of-the-art performances under all metrics on both Flickr30K and MSCOCO datasets, except for zero-shot text-to-image retrieval on Flickr30K, where FILIP achieves competitive performance with SOTA. For zero-shot image-to-text retrieval on MSCOCO dataset, the absolute R@1 of our proposed FILIP is 2.7% higher than ALIGN, which is trained on a much larger dataset.

## 4.4 ABLATION STUDY

**Effectiveness of Each Component.** We study the effectiveness of each component in FILIP, i.e., image/text augmentations and cross-modal late interaction. Experiments are conducted on FILIP<sub>base</sub>, with a filtered subset of YFCC100M as the training dataset (as described in Section 3.3), on both zero-shot retrieval and classification tasks. We measure models’ performance on MSCOCO zero-

Table 3: Results of fine-tuned image-text retrieval on Flickr30K and MSCOCO datasets.

	Flickr30K						MSCOCO					
	image-to-text			text-to-image			image-to-text			text-to-image		
	R@1	R@5	R@10	R@1	R@5	R@10	R@1	R@5	R@10	R@1	R@5	R@10
Unicoder-VL	86.2	96.3	99.0	71.5	90.9	94.9	62.3	87.1	92.8	48.4	76.7	85.9
ImageBERT	87.0	97.6	99.2	73.1	92.6	96.0	66.4	89.8	94.4	50.5	78.7	87.1
UNITER	87.3	98.0	99.2	75.6	94.1	96.8	65.7	88.6	93.8	52.9	79.9	88.0
VILLA	87.9	97.5	98.8	76.3	94.2	96.8	—	—	—	—	—	—
ERNIE-ViL	88.1	98.0	99.2	76.7	93.6	96.4	—	—	—	—	—	—
Oscar	—	—	—	—	—	—	73.5	92.2	96.0	57.5	82.8	89.8
VinVL	—	—	—	—	—	—	75.4	92.9	96.2	58.8	83.5	90.3
ALIGN	95.3	99.8	100.0	84.9	97.4	98.6	77.0	93.5	96.9	59.9	83.3	89.8
ALBEF	95.9	99.8	<b>100.0</b>	85.6	97.5	98.9	77.6	94.3	97.2	60.7	<b>84.3</b>	90.5
Our FILIP	<b>96.6</b>	<b>100.0</b>	<b>100.0</b>	<b>87.1</b>	<b>97.7</b>	<b>99.1</b>	<b>78.9</b>	<b>94.4</b>	<b>97.4</b>	<b>61.2</b>	<b>84.3</b>	<b>90.6</b>

Table 4: Ablation study of different components on pre-training subset of YFCC100M. I2T and T2I are abbreviations for image-to-text and text-to-image retrieval, respectively. “ZS” means zero-shot performance. Underlined numbers have the highest improvements for the corresponding metrics.

Model	MSCOCO				ImageNet
	I2T R@1	I2T R@5	T2I R@1	T2I R@5	ZS Top1
Baseline (ViT-B/32)	25.0	49.5	14.7	34.7	30.4
w/ image augmentation	26.1	51.8	16.5	37.5	32.5
w/ back translation	29.2	55.0	17.9	39.8	33.9
w/ cross-modal late interaction	<u>30.5</u>	<u>55.3</u>	<u>18.5</u>	<u>40.0</u>	<u>34.3</u>
Our FILIP <sub>base</sub>	<b>33.4</b>	<b>60.1</b>	<b>23.0</b>	<b>46.2</b>	<b>37.8</b>

Table 5: Efficiency study of the cross-modal late interaction. “orig” and “late” stand for the contrastive loss based on the original cosine similarity in CLIP and our proposed cross-modal late interaction, respectively. “ZS” means zero-shot performance. We report results for ViT-B/32 trained on filtered YFCC100M with 8 V100 GPUs, with a batch size of 512 per GPU. Training time and memory consumption are tested using the same gradient checkpoint configuration. \* denotes our final setting used in other experiments.

Loss	Embed dim	Embed precision	Token %	Training time (sec/iter)	Memory (MB)	ImageNet ZS Top1
orig (baseline)	512	fp32	-	1.31	14300	30.4
late	512	fp32	100%	2.85	26000	34.6
late	512	fp16	100%	2.67	23468	34.5
late	256	fp16	100%	2.31	22382	<b>35.2</b>
late	256	fp16	50%	1.61	16336	34.5
late*	256	fp16	25%	1.39	16100	34.3

shot image-text retrieval and ImageNet zero-shot classification, which are two effective indicators for the quality of the learned vision-language representations.

Table 4 reports the results. As can be seen, all three components are beneficial for both tasks. Despite the simple design, cross-modal late interaction brings significant performance improvements over the baseline (the vanilla CLIP ViT-B/32), with an absolute R@1 gain of 5.5% (resp. 3.8%) for image-to-text (resp. text-to-image) retrieval on MSCOCO and an absolute top-1 accuracy gain of 3.9% for zero-shot classification on ImageNet. Further improvements are observed when all components are combined together.

**Efficiency Study of Cross-modal Late Interaction.** Since the late interaction mechanism in Section 3.1.1 requires to calculate the similarity between all visual and textual tokens, its efficiency can be a problem when employed in large-scale distributed training. As described in Section 3.1.1, we make several attempts to address the issue. Table 5 shows the efficiency improvement on zero-shot classification on ImageNet when these attempts are applied. As can be seen, these attempts improve



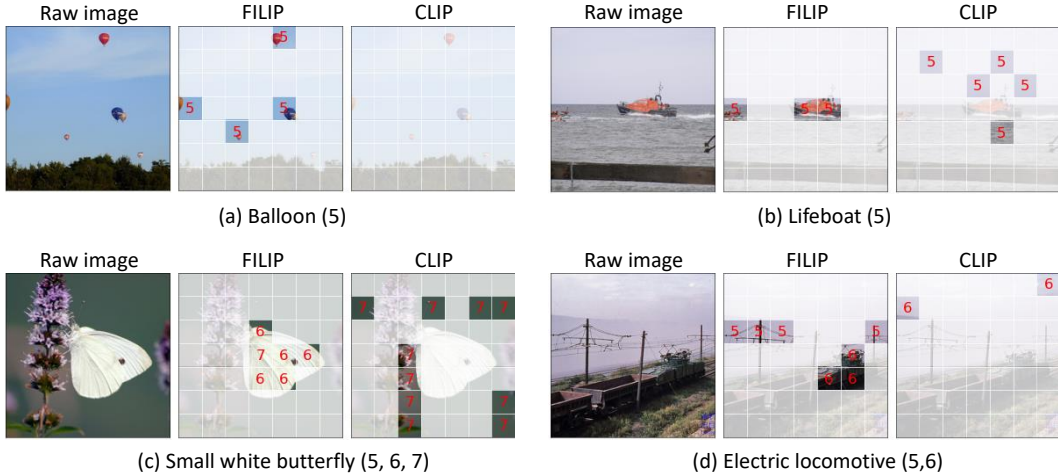


Figure 2: Visualizations of word-patch alignment for 4 classes of the ImageNet dataset and “a photo of a {label}.” is the prompt. Numbers in the parentheses after the class label indicate the location indices of the class label in the tokenized textual sequence. The correct predictions are highlighted by opaque patches with the class label indices in red.

the efficiency of late interaction without accuracy drop. Combining all three attempts achieves only slightly slower training and larger memory consumption than the original loss in CLIP.

#### 4.5 VISUALIZATION OF FINE-GRAINED ALIGNMENT

In this section, we visualize FILIP’s capability of capturing fine-grained cross-modal correspondence using the method of word-patch alignment. To make a fair comparison, we use our  $\text{FILIP}_{\text{base}}$  trained on YFCC100M and CLIP’s ViT-B/32, which are of the same size, for visualization. Each image is patchified to  $7 \times 7$  image patches. More visualization results can be found in Appendix A.3.

**Visualization Method.** The word-patch alignment is performed based on the token-wise similarity between the image patches and textual tokens. Specifically, for the  $k$ -th image patch, the location index of textual token with the largest similarity with it ( $m_k^I$  in Equation (4)) is considered as its predicted label, and is placed at the center of it. Take class “balloon” as an example. There are 8 tokens in the tokenized textual sequence “[BOS] a photo of a balloon. [EOS]”, and the location index of the class label “balloon” is “5”. Note that one class label may be tokenized to more than one token. Location indices of textual tokens corresponding to the class label are highlighted in red, while the others are marked in white. A desired model that learns fine-grained representations would predict image patches of the target object to red indices.

**Observations.** Figure 2 shows the word-patch alignment results for FILIP and CLIP on 4 classes from the ImageNet dataset. As can be seen, FILIP exhibits the finer-grained understanding of an image in the following aspects. (i) A single object: From the visualization of class “small white butterfly”, the image patches covering the object are all classified correctly; (ii) Same object in different shapes: From the visualizations of class “balloon” and “lifeboat”, image patches corresponding to all target objects with different shapes and locations are correctly classified; (iii) Key Components of an object: For class “electric locomotive”, there are two key components crucial to correctly classifying the image, i.e., “electric” and “locomotive”, whose corresponding textual token indices are “5” and “6”, respectively. As can be seen, image patches matching these two key components are respectively correctly classified. On the other hand, CLIP can not correctly align image patches with corresponding textual tokens. Compared with Kim et al. (2021) which uses an extra optimal transport to align the textual word and image patch distributions, the word-patch alignment can be simply automatically learned by our method.

## 5 CONCLUSION AND FUTURE WORK

This paper introduces FILIP, a simple yet generic framework towards fine-grained vision-language pre-training. By using a token-wise maximum similarity, our method learns fine-grained represen-

tation for patches in the images and words in the sentences. While it achieves competitive results against several large-scale multi-modal pre-training on various downstream tasks, both its architecture and training procedure can still be optimized to improve its performance. In the future, a more advanced image encoder as well as a well-designed interaction layer can be used to boost the performance. Furthermore, we can further add more masked language/image loss to support more generation tasks. To this end, we hope to extend FILIP as a generic and unified interface for solving a large variety of vision-language tasks.

## REFERENCES

- Tom B Brown, Benjamin Mann, Nick Ryder, Melanie Subbiah, Jared Kaplan, Prafulla Dhariwal, Arvind Neelakantan, Pranav Shyam, Girish Sastry, Amanda Askell, et al. Language models are few-shot learners. In *Advances in neural information processing systems*, 2020.
- Soravit Changpinyo, Piyush Sharma, Nan Ding, and Radu Soricut. Conceptual 12M: Pushing web-scale image-text pre-training to recognize long-tail visual concepts. In *IEEE/CVF Conference on Computer Vision and Pattern Recognition*, 2021.
- Tianqi Chen, Bing Xu, Chiyuan Zhang, and Carlos Guestrin. Training deep nets with sublinear memory cost. preprint arXiv:1604.06174, 2016.
- Yen-Chun Chen, Linjie Li, Licheng Yu, Ahmed El Kholy, Faisal Ahmed, Zhe Gan, Yu Cheng, and Jingjing Liu. Uniter: Universal image-text representation learning. In *European conference on computer vision*, pp. 104–120. Springer, 2020.
- Ekin D Cubuk, Barret Zoph, Dandelion Mane, Vijay Vasudevan, and Quoc V Le. Autoaugment: Learning augmentation strategies from data. In *Proceedings of the IEEE/CVF Conference on Computer Vision and Pattern Recognition*, pp. 113–123, 2019.
- Jacob Devlin, Ming-Wei Chang, Kenton Lee, and Kristina Toutanova. Bert: Pre-training of deep bidirectional transformers for language understanding. In *Annual Conference of the North American Chapter of the Association for Computational Linguistics*, 2019.
- Ming Ding, Zhuoyi Yang, Wenyi Hong, Wendi Zheng, Chang Zhou, Da Yin, Junyang Lin, Xu Zou, Zhou Shao, Hongxia Yang, et al. Cogview: Mastering text-to-image generation via transformers. *arXiv preprint arXiv:2105.13290*, 2021.
- Xiao Dong, Xunlin Zhan, Yangxin Wu, Yunchao Wei, Xiaoyong Wei, Minlong Lu, and Xiaodan Liang. M5product: A multi-modal pretraining benchmark for e-commercial product downstream tasks. Preprint arXiv:2109.04275, 2021.
- Alexey Dosovitskiy, Lucas Beyer, Alexander Kolesnikov, Dirk Weissenborn, Xiaohua Zhai, Thomas Unterthiner, Mostafa Dehghani, Matthias Minderer, Georg Heigold, Sylvain Gelly, et al. An image is worth 16x16 words: Transformers for image recognition at scale. In *International Conference on Learning Representations*, 2020.
- Zhe Gan, Yen-Chun Chen, Linjie Li, Chen Zhu, Yu Cheng, and Jingjing Liu. Large-scale adversarial training for vision-and-language representation learning. *arXiv preprint arXiv:2006.06195*, 2020.
- Andreas Griewank and Andrea Walther. Algorithm 799: revolve: an implementation of checkpointing for the reverse or adjoint mode of computational differentiation. *ACM Transactions on Mathematical Software (TOMS)*, 26(1):19–45, 2000.
- Elad Hoffer, Tal Ben-Nun, Itay Hubara, Niv Giladi, Torsten Hoefler, and Daniel Soudry. Augment your batch: Improving generalization through instance repetition. In *Proceedings of the IEEE/CVF Conference on Computer Vision and Pattern Recognition*, pp. 8129–8138, 2020.
- Zhicheng Huang, Zhaoyang Zeng, Yupan Huang, Bei Liu, Dongmei Fu, and Jianlong Fu. Seeing out of the box: End-to-end pre-training for vision-language representation learning. In *IEEE/CVF Conference on Computer Vision and Pattern Recognition*, pp. 12976–12985, 2021.

- Chao Jia, Yinfei Yang, Ye Xia, Yi-Ting Chen, Zarana Parekh, Hieu Pham, Quoc V Le, Yunhsuan Sung, Zhen Li, and Tom Duerig. Scaling up visual and vision-language representation learning with noisy text supervision. In *International Conference on Machine Learning*, 2021.
- Omar Khattab and Matei Zaharia. Colbert: Efficient and effective passage search via contextualized late interaction over bert. In *International ACM SIGIR Conference on Research and Development in Information Retrieval*, pp. 39–48, 2020.
- Wonjae Kim, Bokyung Son, and Ildoo Kim. Vilt: Vision-and-language transformer without convolution or region supervision. In *International Conference on Machine Learning*, 2021.
- Alex Krizhevsky, Ilya Sutskever, and Geoffrey E Hinton. Imagenet classification with deep convolutional neural networks. In *Advances in neural information processing systems*, volume 25, pp. 1097–1105, 2012.
- Gen Li, Nan Duan, Yuejian Fang, Ming Gong, and Daxin Jiang. Unicoder-vl: A universal encoder for vision and language by cross-modal pre-training. In *Proceedings of the AAAI Conference on Artificial Intelligence*, volume 34, pp. 11336–11344, 2020a.
- Junnan Li, Ramprasaath R. Selvaraju, Akhilesh Deepak Gotmare, Shafiq Joty, and Steven Xiong, Caiming and Hoi. Align before fuse: Vision and language representation learning with momentum distillation. Technical Report arXiv:2107.07651, 2021a.
- Liunian Harold Li, Mark Yatskar, Da Yin, Cho-Jui Hsieh, and Kai-Wei Chang. Visualbert: A simple and performant baseline for vision and language. Preprint arXiv:1908.03557, 2019.
- Wei Li, Can Gao, Guocheng Niu, Xinyan Xiao, Hao Liu, Jiachen Liu, Hua Wu, and Haifeng Wang. Unimo: Towards unified-modal understanding and generation via cross-modal contrastive learning. In *Annual Meeting of the Association for Computational Linguistics*, 2021b.
- Xiujun Li, Xi Yin, Chunyuan Li, Pengchuan Zhang, Xiaowei Hu, Lei Zhang, Lijuan Wang, Houdong Hu, Li Dong, Furu Wei, et al. Oscar: Object-semantics aligned pre-training for vision-language tasks. In *European Conference on Computer Vision*, pp. 121–137. Springer, 2020b.
- Junyang Lin, Rui Men, An Yang, Chang Zhou, Ming Ding, Yichang Zhang, Peng Wang, Ang Wang, Le Jiang, Xianyan Jia, et al. M6: A chinese multimodal pretrainer. Preprint arXiv:2103.00823, 2021.
- Tsung-Yi Lin, Michael Maire, Serge Belongie, James Hays, Pietro Perona, Deva Ramanan, Piotr Dollár, and C Lawrence Zitnick. Microsoft coco: Common objects in context. In *European conference on computer vision*, pp. 740–755. Springer, 2014.
- I. Loshchilov and F. Hutter. Sgdr: Stochastic gradient descent with warm restarts. *ICLR 2017 (5th International Conference on Learning Representations)*, 2016.
- Jiasen Lu, Dhruv Batra, Devi Parikh, and Stefan Lee. Vilbert: pretraining task-agnostic vision-linguistic representations for vision-and-language tasks. In *International Conference on Neural Information Processing Systems*, pp. 13–23, 2019.
- Paulius Micikevicius, Sharan Narang, Jonah Alben, Gregory Diamos, Erich Elsen, David Garcia, Boris Ginsburg, Michael Houston, Oleksii Kuchaiev, Ganesh Venkatesh, et al. Mixed precision training. In *International Conference on Learning Representations*, 2018.
- Bryan A Plummer, Liwei Wang, Chris M Cervantes, Juan C Caicedo, Julia Hockenmaier, and Svetlana Lazebnik. Flickr30k entities: Collecting region-to-phrase correspondences for richer image-to-sentence models. In *IEEE international conference on computer vision*, pp. 2641–2649, 2015.
- Di Qi, Lin Su, Jia Song, Edward Cui, Taroon Bharti, and Arun Sacheti. Imagebert: Cross-modal pre-training with large-scale weak-supervised image-text data. *arXiv preprint arXiv:2001.07966*, 2020.
- Alec Radford, Karthik Narasimhan, Tim Salimans, and Ilya Sutskever. Improving language understanding by generative pre-training. 2018.

- Alec Radford, Jeffrey Wu, Rewon Child, David Luan, Dario Amodei, Ilya Sutskever, et al. Language models are unsupervised multitask learners. *OpenAI blog*, 1(8):9, 2019.
- Alec Radford, Jong Wook Kim, Chris Hallacy, Aditya Ramesh, Gabriel Goh, Sandhini Agarwal, Girish Sastry, Amanda Askell, Pamela Mishkin, Jack Clark, et al. Learning transferable visual models from natural language supervision. Preprint arXiv:2103.00020, 2021.
- Colin Raffel, Noam Shazeer, Adam Roberts, Katherine Lee, Sharan Narang, Michael Matena, Yanqi Zhou, Wei Li, and Peter J Liu. Exploring the limits of transfer learning with a unified text-to-text transformer. *Journal of Machine Learning Research*, 21:1–67, 2020.
- Aditya Ramesh, Mikhail Pavlov, Gabriel Goh, Scott Gray, Chelsea Voss, Alec Radford, Mark Chen, and Ilya Sutskever. Zero-shot text-to-image generation. Preprint arXiv:2102.12092, 2021.
- Shaoqing Ren, Kaiming He, Ross Girshick, and Jian Sun. Faster r-cnn: Towards real-time object detection with region proposal networks. *Advances in neural information processing systems*, 28: 91–99, 2015.
- Ikuro Sato, Hiroki Nishimura, and Kensuke Yokoi. Apac: Augmented pattern classification with neural networks. Technical Report arXiv:1505.03229, 2015.
- Ramprasaath R Selvaraju, Michael Cogswell, Abhishek Das, Ramakrishna Vedantam, Devi Parikh, and Dhruv Batra. Grad-cam: Visual explanations from deep networks via gradient-based localization. In *IEEE international conference on computer vision*, pp. 618–626, 2017.
- Rico Sennrich, Barry Haddow, and Alexandra Birch. Improving neural machine translation models with monolingual data. In *Annual Meeting of the Association for Computational Linguistics (Volume 1: Long Papers)*, pp. 86–96, 2016a.
- Rico Sennrich, Barry Haddow, and Alexandra Birch. Neural machine translation of rare words with subword units. In *Annual Meeting of the Association for Computational Linguistics (Volume 1: Long Papers)*, pp. 1715–1725, 2016b.
- Piyush Sharma, Nan Ding, Sebastian Goodman, and Radu Soricut. Conceptual captions: A cleaned, hypernymed, image alt-text dataset for automatic image captioning. In *Annual Meeting of the Association for Computational Linguistics (Volume 1: Long Papers)*, pp. 2556–2565, 2018.
- Bart Thomee, David A Shamma, Gerald Friedland, Benjamin Elizalde, Karl Ni, Douglas Poland, Damian Borth, and Li-Jia Li. Yfcc100m: The new data in multimedia research. *Communications of the ACM*, 59(2):64–73, 2016.
- Yonglong Tian, Dilip Krishnan, and Phillip Isola. Contrastive multiview coding. In *Computer Vision—ECCV 2020: 16th European Conference*, pp. 776–794. Springer, 2020.
- Hugo Touvron, Matthieu Cord, Matthijs Douze, Francisco Massa, Alexandre Sablayrolles, and Hervé Jégou. Training data-efficient image transformers & distillation through attention. In *International Conference on Machine Learning*, pp. 10347–10357. PMLR, 2021.
- Zirui Wang, Jiahui Yu, Adams Wei Yu, Zihang Dai, Yulia Tsvetkov, and Yuan Cao. Simvlm: Simple visual language model pretraining with weak supervision. Preprint arXiv:2108.10904, 2021.
- Qizhe Xie, Zihang Dai, Eduard Hovy, Thang Luong, and Quoc Le. Unsupervised data augmentation for consistency training. In *Advances in Neural Information Processing Systems*, volume 33, 2020a.
- Qizhe Xie, Minh-Thang Luong, Eduard Hovy, and Quoc V Le. Self-training with noisy student improves imagenet classification. In *Proceedings of the IEEE/CVF Conference on Computer Vision and Pattern Recognition*, pp. 10687–10698, 2020b.
- Yang You, Jing Li, Sashank Reddi, Jonathan Hseu, Sanjiv Kumar, Srinadh Bhojanapalli, Xiaodan Song, James Demmel, Kurt Keutzer, and Cho-Jui Hsieh. Large batch optimization for deep learning: Training bert in 76 minutes. In *International Conference on Learning Representations*, 2020.

- Fei Yu, Jiji Tang, Weichong Yin, Yu Sun, Hao Tian, Hua Wu, and Haifeng Wang. Ernie-vil: Knowledge enhanced vision-language representations through scene graphs. In *Proceedings of the AAAI Conference on Artificial Intelligence*, volume 35, pp. 3208–3216, 2021.
- Xunlin Zhan, Yangxin Wu, Xiao Dong, Yunchao Wei, Minlong Lu, Yichi Zhang, Hang Xu, and Xiaodan Liang. Product1m: Towards weakly supervised instance-level product retrieval via cross-modal pretraining. In *International Conference on Computer Vision*, 2021.
- Pengchuan Zhang, Xiujun Li, Xiaowei Hu, Jianwei Yang, Lei Zhang, Lijuan Wang, Yejin Choi, and Jianfeng Gao. Vinvl: Revisiting visual representations in vision-language models. In *IEEE/CVF Conference on Computer Vision and Pattern Recognition*, pp. 5579–5588, 2021.

## A APPENDIX

### A.1 DATASETS SUMMARY

Table 6 shows the number of image-text pairs of each datasets used in different pre-training methods.

Table 6: Number of image-text pairs used in the pre-training of FILIP, CLIP and ALIGN.

#	FILIP				CLIP	ALIGN
	CC3M	CC12M	YFCC100M	FILIP300M	(Radford et al., 2021)	(Jia et al., 2021)
	3M	10M	26M	300M	400M	1800M

### A.2 DETAILED EXPERIMENTAL SETTINGS

Table 7: The architecture parameters for FILIP models.

Model	Embedding dimension	Input resolution	Image Encoder			Text Encoder		
			#layers	width	#heads	#layers	width	#heads
FILIP <sub>base</sub>	256	224 × 224	12	768	12	12	512	8
FILIP <sub>large</sub>	256	224 × 224	24	1024	16	12	768	12

**Model Architectures.** We follow the same architecture design as CLIP, for both FILIP<sub>base</sub> and FILIP<sub>large</sub>, except that we reduce the embedding dimension from 512/768 to 256 for the efficiency of loss computation. Table 7 describes the details of architectures.

**Details for Pre-training and Hyperparameters.** For the implementation of the contrastive loss, following CLIP (Radford et al., 2021) and ALIGN (Jia et al., 2021), we also set the temperature in the softmax function to be a learnable parameter and initialize it as 0.07. For the pre-training, we use the LAMB optimizer implemented by the cybertronai’s open-source repository (<https://github.com/cybertronai/pytorch-lamb>). For the learning rate scheduler, we first assign a base learning rate and then linearly warm it up to the peak learning rate according to the effective total batch size by a square root strategy,  $peak\_lr = base\_lr \times \sqrt{\frac{total\_bs}{512}}$ . We note that a large weight decay is crucial to stabilize training and improve generalization. Specifically, we found that the training stability is a challenging issue when applying mix-precision training to large-scale models, i.e., the training is extremely unstable and the NaN loss easily happens. Recent works DALL-E (Ramesh et al., 2021) and Cogview (Ding et al., 2021) also notice this issue and provide their solutions. However, we found that simply increasing the weight decay and applying the trick of removing the weight decay of specific parameters as described in Section 4.1 work for our case. The base learning rate and weight decay are selected manually via observing the performance at the early training stage. Table 8 summarizes the common hyperparameters and Table 9 shows the model- and dataset-specific hyperparameters for FILIP pre-training.

Table 8: Common hyperparameters used for FILIP pre-training.

Hyperparameter	Value
Vocabulary size	49408
Initial temperature	0.07
LAMB $\beta_1$	0.9
LAMB $\beta_2$	0.999
LAMB $\epsilon$	$10^{-4}$
Warm-up iters	3000
Training epochs	30

Table 9: Model- and dataset-specific hyperparameters used for FILIP pre-training. Numbers in batch size represent the total batch size across all workers and are calculated as: batch size per GPU  $\times$  #GPUs. FILIP340M is the combination of FILIP300M, YFCC100M, CC12M and CC3M.

Model	Dataset	Batch size	Base LR	Weight decay
FILIP <sub>base</sub>	YFCC100M	$1024 \times 8$	$6 \times 10^{-3}$	3e-2
FILIP <sub>base</sub>	FILIP340M	$320 \times 128$	$2 \times 10^{-3}$	3e-3
FILIP <sub>large</sub>	FILIP340M	$160 \times 192$	$8 \times 10^{-4}$	3e-3

**Details for Image-text Retrieval.** Following previous works (Jia et al., 2021; Li et al., 2021a), for Flickr30K, we test on the 1K test set with or without fine-tuning on the 30K training set, while for MSCOCO, we test on the 5K test set with or without fine-tuning on the 113K training set. We use the similarity between image and text for ranking and use the contrastive loss for fine-tuning. Since there are multiple texts for each image in these two datasets, we change the ground-truth label of contrastive loss to consider multiple positives, by assigning a probability of  $1/\#\text{positive}$  to each positive following ALBEF (Li et al., 2021a). Besides, we also use prompts during evaluation for both datasets, see Appendix A.4 for details. Table 10 shows the hyperparameters for image-text retrieval fine-tuning.

Table 10: Hyperparameters used for image-text retrieval fine-tuning.

Hyperparameter	Value
Image size	$392 \times 392$
Training epochs	3
Optimizer	LAMB
Batch size	5120
Base LR	$2 \times 10^{-4}$
Weight decay	$3 \times 10^{-4}$

### A.3 MORE VISUALIZATIONS OF WORD-PATCH ALIGNMENT AND GRAD-CAM HEATMAPS

In Figure 3, we visualize the cross-modal alignment of the proposed method for more images, in terms of both word-patch alignment as described in Section 4.5 and Grad-CAM heatmaps (Selvaraju et al., 2017). We compute the Grad-CAM heatmaps based on the average self-attention maps over the image patches classified to targeted textual tokens (i.e., the textual token(s) corresponding to the class label in the ImageNet dataset) in the last layer of the image encoder. We average the heatmaps over all attention heads. As can be seen, our proposed model learns meaningful alignment between image patches and textual tokens.

### A.4 PROMPT TEMPLATES FOR DOWNSTREAM TASKS

**Image Classification.** Table 11 shows the prompt templates for different image classification datasets in the form of “[prefix] {label}, [category description]. [suffix].” in Equation (6). There are three components to be determined in the template, i.e., the prefix, the category description and the suffix. For each component, we select several well-performed ones for each dataset. Then we use the full combinations of all three components as the set of prompt templates for ensemble. For instance, we use 5 prefixes, no category descriptions, and 6 suffixes for dataset ImageNet. Then the total number of prompt templates for this dataset is:  $5 \times 1 \times 6 = 30$ .

**Image-text Retrieval.** Following CLIP (Radford et al., 2021), we use prompt in zero-shot image-text retrieval for both Flickr30K and MSCOCO datasets. The prompt is selected by the same rule as described in Section 3.1.2, except that we do not use “[category description]” here. Table 12 shows the prompt templates for zero-shot image-text retrieval on Flickr30K and MSCOCO datasets.

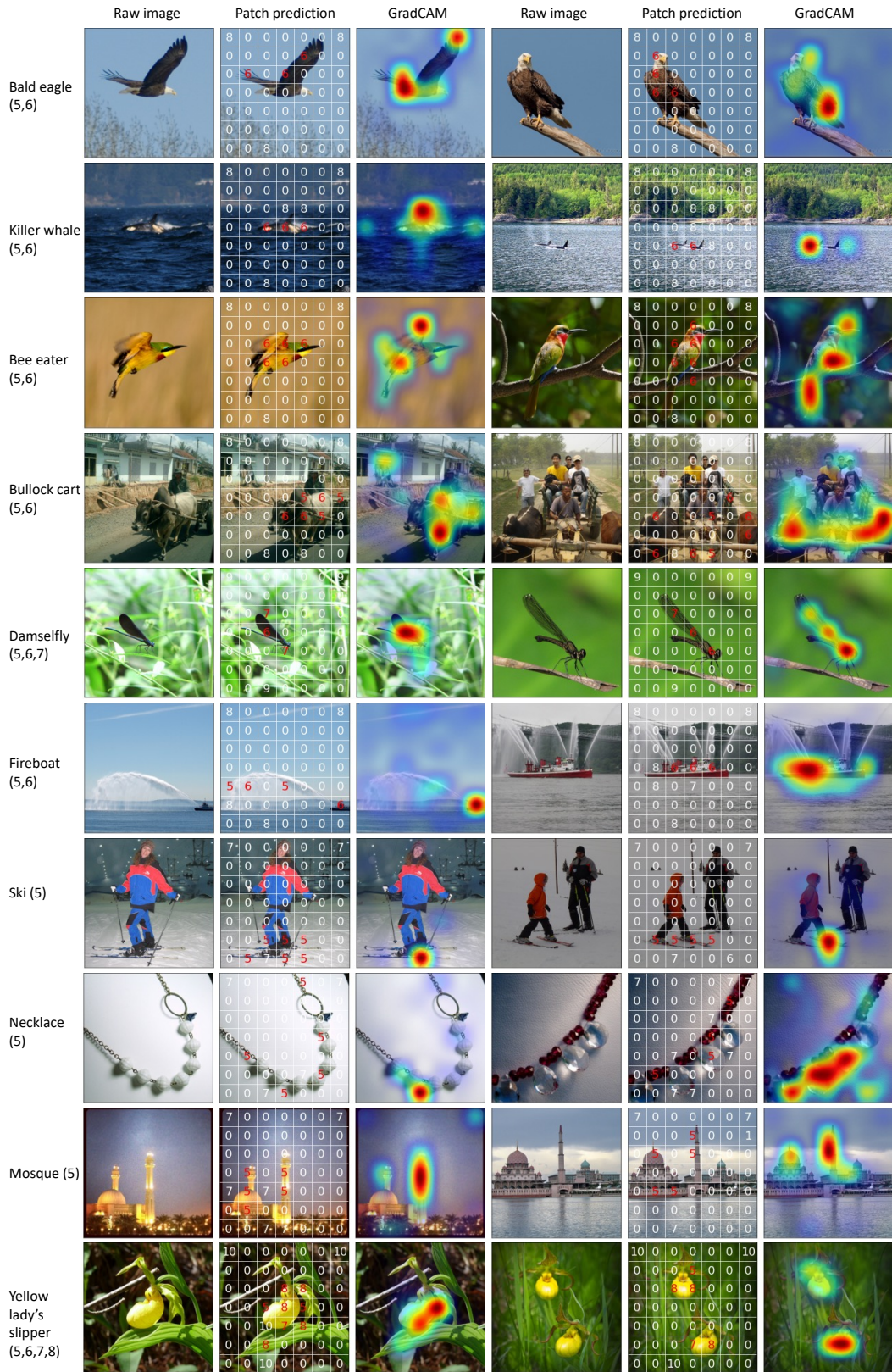


Figure 3: More visualizations on different classes of ImageNet dataset. Numbers in the parentheses after the class label indicate the location indices of class label in the tokenized textual sequence.



Table 11: Prompt templates used for 12 downstream image classification tasks.

Dataset	Prefix	Category description	Suffix
CIFAR10	“a photo of a”, “a jpeg photo of a”, “a painting of a”, “itap of a”, “graffiti of a”, “a cartoon”, “a doodle”	None	None, “It’s common in daily life”, “It’s cute”, “It’s ugly”, “It’s weird”, “Hope you like it”
CIFAR100	“a jpeg photo of a”, “a painting of a”, “a good photo of a”, “a bad photo of a”, “a photo of a”, “itap of a”, “a rendering of a”	None	None, “It’s common in daily life”, “It’s beautiful”, “It’s ugly”, “I like it”, “I take it today”
Caltech101	“a photo of a”, “a cropped photo of a”, “a good photo of a”, “a bad photo of a”	None	None, “I like it”, “I hate it”, “It’s ugly”, “It’s cute”
Stanford-Car	“a photo of a”, “a close-up photo of a”, “a good photo of a”, “a bad photo of a”	“a type of car”, “a type of automobile”	“I like it”, “It belongs to my friend”, “It’s brand new”, “It’s popular recently”, “It’s important to me”, “I take it today”
Flowers102	“a photo of a (many)”, “a rendering of a (many)”, “itap of a (many)”	“a type of flower”, “a type of bloom”	“It’s beautiful”, “It’s from my best friend”, “It gives out a sweet perfume/fragrance”
ImageNet	“a photo of a”, “a good photo of a”, “a bad photo of a”, “a close-up photo of a”, “itap of a”	None	“I like it”, “It’s common in daily life”, “It’s not common in daily life”, “It’s ugly”, “It’s cute”, “It’s beautiful”
Food101	“a photo of my”, “a close-up photo of my”, “itap of my”	“a type of food”, “a type of nourishment”	“I made it today”, “I like it”, “I hate it”, “It’s delicious”, “It’s with nice flavour”, “It’s with terrible flavour”, “It’s popular recently”
SUN397	“a photo of a”, “a good photo of a”, “a bad photo of a”, “a bright photo of a”, “a dark photo of a”, “a black and white photo of a”, “a nice scene of a”, “a terrible scene of a”	None	None, “I like it”, “I hate it”, “It’s beautiful”, “It’s common in daily life”, “It’s important to me”
DTD	“itap of a”, “a close-up photo of a”	“texture”, “surface”, “material”	None, “It’s out of style”, “It’s popular in old days”, “It’s ugly”, “It’s beautiful”
Aircrafts	“a photo of the”, “a close-up photo of the”, “a good photo of the”, “a pixelated photo of the”	“a type of plane”, “a type of aircraft”, “a type of airliner”	None, “I like it”, “It’s important to me”, “I take it today”, “Hope you like it”
Oxford Pet	“a photo of my”, “a low resolution photo of my”, “a good photo of my”	“a type of pet”, “a type of dog or cat”	None, “It’s cute”, “It’s important to me”, “I like it”, “It’s beautiful”
EuroSAT	“a photo of a”, “a painting of a”, “a cropped photo of a”, “a good photo of a”, “a blurry photo of a”	None, “an example of aerial or satellite images”	None, “I like it”, “It’s taken from an aircraft or some flying object”, “It’s collected by imaging satellites”

Table 12: Prompt templates used for zero-shot image-text retrieval on Flickr30K and MSCOCO datasets.

Dataset	Task	Prefix	Suffix
Flickr30K	image-to-text retrieval	“a good photo of the”	“I hate it.”
	text-to-image retrieval	“a good photo of”	None
MSCOCO	image-to-text retrieval	“a good photo of”	“It is ugly.”
	text-to-image retrieval	None	None